

Comparison of Mixing Model Performance for Nonpremixed Turbulent Reactive Flow

S. SUBRAMANIAM* and S. B. POPE

Sibley School of Mechanical and Aerospace Engineering, Cornell University, Ithaca, New York 14853-7501

A spatially inhomogeneous model problem for studying turbulent nonpremixed reacting flow with reversible reaction is proposed, which admits stationary solutions that are periodic in physical space. The thermochemical state of the fluid is characterized by two composition variables: mixture fraction $\xi(x, t)$ and reaction progress variable $Y(x, t)$. A linear gradient in the mean mixture fraction field is imposed in the x_2 direction, so that, in a forced stationary velocity field, the mixture fraction field attains statistical stationarity. The reaction progress variable $Y(x, t)$ is statistically homogeneous in x_1 and x_3 , and is statistically periodic in x_2 . The flow is called *periodic reaction zones*. The solutions are parametrized by the Damköhler number and the reaction zone thickness parameter. At sufficiently high Damköhler number there is stable reaction, but as the Damköhler number is decreased below a critical value, global extinction occurs. The range of parameter values is chosen such that the model problem reproduces important phenomena such as stable near-equilibrium reaction, local extinction, and global extinction. Monte Carlo simulations are performed to solve for the joint probability density function of velocity, turbulent frequency, and composition. The predictions for critical Damköhler number are compared for two different mixing models: the interaction by exchange with the mean (IEM) model, and the Euclidean Minimum Spanning Tree (EMST) model. The results obtained using the simpler conditional moment closure (CMC) model are also presented for comparison. The model problem is formulated to permit direct numerical simulations (DNS) using pseudo-spectral methods, which require periodic boundary conditions. The DNS study of this model problem, which is reported in a separate publication, provides additional insight into the phenomenon of extinction in inhomogeneous turbulent reactive flows. © 1999 by The Combustion Institute

NOMENCLATURE

B	thermochemical parameter	l	lengthscale of the turbulence, $\equiv u'^3/\epsilon$
B_v	EMST model constant	L	computational box length in x_2 direction
C_0	model constant in simplified Langevin model	M	number of multiple independent simulations
C_3	model constant in turbulent frequency model	N	number of particles
C_ϕ	model constant in scalar variance equation	N_{pc}	number of particles per cell
D	number of composition variables	q	$Y_e - Q$, departure from equilibrium of the conditional mean of Y
Da	Damköhler number	Q	mean of Y conditioned on ξ
Da_u	upper estimate of the critical Damköhler number	R_λ	Taylor-scale Reynolds number
Da_l	lower estimate of the critical Damköhler number	S	reaction rate
e_Q	term in the CMC closure	S_ω	source term in turbulent frequency equation
$e_{\bar{y}}$	term in the CMC closure	t	time
$E.I.$	extinction index	T_s	simulation time
f	thermochemical function	T_t	transport timescale
g	thermochemical function	u, u'	fluctuating velocity field, standard deviation of velocity fluctuations
k	turbulent kinetic energy	U, U	velocity
		w	importance weight
		W, dW	Wiener process, increment thereof
		x	Cartesian vector in physical space

*Corresponding author. E-mail shankar@lanl.gov

X	particle position
Y	reaction progress variable
Y_e	equilibrium value of the reaction progress variable
y	$Y_e - Y$, departure from equilibrium of the reaction progress variable
\bar{y}	$Y - Q$, departure of Y from its conditional mean

Greek Symbols

α	model parameter controlling the variance decay rate
γ_t	eddy diffusivity
Γ	molecular diffusivity
$\Delta\xi_e$	mixture fraction scale associated with equilibrium function
	curvature in ξ space
$\Delta\xi_L$	jump in mean mixture fraction over computational box of length L
$\Delta\xi_r$	reaction zone thickness in mixture fraction space
$\Delta\xi_{r_{ss}}$	reaction zone thickness in mixture fraction space as defined in the self-similar thermochemistry
ϵ	mean dissipation rate of turbulence
η	sample space variable of ξ
Θ	mixing model term
ν	edge index
ξ	mixture fraction
ξ'	standard deviation of the mixture fraction
$\check{\xi}$	mixture fraction fluctuation field
$\hat{\xi}_r$	reaction zone thickness parameter $\equiv \Delta\xi_r/\xi'$
$\hat{\xi}_{r_{ss}}$	reaction zone thickness parameter as defined in the self-similar thermochemistry
σ	model parameter in particle ω equation
τ	time-scale, turbulence time-scale
τ^*	characteristic chemical reaction timescale
τ_ϕ	characteristic mixing timescale
τ_c	thermochemical parameter controlling the magnitude of the reaction rate
ϕ, Φ	composition

$\chi, \langle\chi\rangle$	scalar dissipation, mean scalar dissipation
$\omega, \langle\omega\rangle$	particle turbulent frequency, mean turbulent frequency

Subscripts

R	quantity associated with the reaction zone
T	quantity associated with the tree equilibrium
e	equilibrium
i, j, m, n	particle index in ensemble, index of Cartesian coordinate
k	index of Cartesian coordinate
l	lean, lower value of interval
pc	per cell
r	rich
s	stoichiometric
ss	statistically stationary value, or value in self-similar thermochemistry
β	index of composition variable
ν	edge index
ϕ	quantity associated with composition
$[]_T$	time averaged quantity
$[]_L$	spatially averaged quantity

Superscripts

i	particle index in ensemble
β	index of composition variable
\wedge	scaled quantity
'	fluctuating quantity, standard deviation thereof
"	second derivative

INTRODUCTION

Prediction of the extinction characteristics of turbulent nonpremixed flames is an important and challenging area of current research. An important parameter in nonpremixed flames is the Damköhler number:

$$Da \equiv \tau_\phi/\tau^*, \quad (1)$$

which is the ratio of the characteristic mixing timescale τ_ϕ to the characteristic chemical timescale τ^* .

When the Damköhler number is very large, the fluid composition almost everywhere in the

physical domain is very close to chemical equilibrium because reaction is rapid compared to the time taken to mix with neighboring fluid. In such situations models based on the equilibrium assumption or those based on small departures from equilibrium may be used with confidence. However, in most turbulent flames there is a range of turbulent timescales (or, in other words, mixing timescales) and there is a corresponding range of Damköhler numbers. As the Damköhler number decreases at any given physical location (as a result of an increase in the local scalar dissipation rate), departures from equilibrium become significant and may result in local extinction. If the Damköhler number is too small to sustain stable combustion in a sufficiently large fraction of the fluid volume, global extinction occurs.

Experiments on piloted jet diffusion flames by Masri et al. [1] provide direct evidence of these phenomena. Clearly, modeling such jet diffusion flames based on equilibrium or near-equilibrium assumptions is questionable. Computations of piloted jet flames using the PDF transport equation approach have been performed with finite-rate chemistry [2–4]. While the calculations of Norris and Pope [4] are successful in predicting the jet velocity at which global extinction occurs, the details of local extinction are not well represented. These discrepancies were attributed to three factors: deficiencies in the mixing model, differential diffusion effects which were neglected, and experimental error. In spite of establishing the overall success of the PDF approach in modeling turbulent nonpremixed flames, these calculations highlight the need for a better understanding of such reactive flows.

While the comparison of model predictions with experimental data is the ultimate test of a model, it is difficult to pinpoint the model deficiencies in comparisons with experiment for several reasons. In real flows there are many complex coupled processes and it is difficult to isolate the effects of the physical process being modeled. The modeled terms, e.g., Lagrangian time series of composition or conditional scalar dissipation, are often not amenable to direct measurement.

On the other hand direct numerical simulations (DNS) can be used to perform controlled

numerical experiments on simple turbulent reactive flows and all flow properties of interest can be extracted. Since many features characteristic of turbulent flames can be represented in a simpler model problem, a satisfactory model for turbulent flames should perform comparably in a simpler turbulent reactive flow. Modeling deficiencies may be identified more easily in the model problem setting. Furthermore, the model behavior in the simpler flow problem can be used to gain valuable insight into the model performance in real turbulent flames. In fact, such computations of practical combusting flows are an ongoing part of this research effort and this work is intended as an important complement thereof.

The present contribution constitutes an intermediate step to the comparison of model predictions with DNS. The objectives of the present work are two-fold: the first is to construct a simple inhomogeneous, nonpremixed reactive flow model problem that is amenable to DNS; the second is to study the effect of PDF models of molecular mixing on model predictions over a range of flow conditions including those close to extinction. In particular, it is of interest to determine whether the new principle of localness [5, 6] required of mixing models enables a more accurate representation of mixing in reactive flows.

In general a constant-density, constant-diffusivity (equal for all species), nonpremixed turbulent reactive flow can be characterized by a Reynolds number (say the Taylor-scale Reynolds number R_λ), Damköhler number and a reaction zone thickness parameter defined as

$$\hat{\xi}_r \equiv \Delta \xi_r / \xi', \quad (2)$$

where $\Delta \xi_r$ is the characteristic width of the reaction zone in mixture-fraction space and ξ' is the r.m.s. mixture fraction. These parameters may be functions of space and time.

In order to obtain a quantitative description of extinction in this $(R_\lambda, Da, \hat{\xi}_r)$ parameter space with finite computer resources, the model problem is necessarily very simple both in terms of flow and thermochemistry. The velocity field is constant-density, statistically stationary, homogeneous isotropic turbulence. A simple thermochemical model for one-step reversible reac-

tion is employed, with the thermochemical state of the fluid described by two variables: the mixture fraction and reaction progress variable. It is advantageous to consider a model problem which admits statistically stationary solutions. This removes the temporal dependence of the parameters and also allows study of flow characteristics independent of the influence of initial conditions. Even with these simplifications, a statistical description of extinction using numerical simulations is subject to statistical variability and is dependent on the duration of the simulation [7].

In previous studies of extinction by Lee and Pope [7], stationarity was achieved by artificially forcing the mixture fraction field, but in this model problem stationarity is achieved by imposing a linear mean gradient in the mixture fraction. The mean gradient in mixture fraction also results in a “flame brush,” which is a more realistic case than that considered in Lee and Pope [7]. The flow under consideration has statistical inhomogeneity only in the reaction progress variable and only in the spatial dimension along which the linear mean gradient in mixture fraction is imposed.

At high Reynolds number, the extinction characteristics are expected to become independent of the Reynolds number. One of the goals of these simulations is a characterization of global extinction by means of a stability diagram in $Da - \hat{\xi}_r$ parameter space similar to that shown in Lee and Pope [7].

The following section describes the model problem and governing equations. This is followed by a description of the reaction rates used in this study. Then the section on turbulent combustion models describes the conditional moment closure (CMC) model and the PDF turbulent combustion models which are compared in this work. Results for a range of parameters using the different turbulent combustion models are then presented. It is found that the models are in good agreement for large values of the reaction zone thickness parameter $\hat{\xi}_r$, but there are significant differences for small values of $\hat{\xi}_r$. These differences are discussed in the light of the modeling assumptions inherent in each model and are summarized in the final section.

PERIODIC REACTION ZONES MODEL PROBLEM

Multiple parallel slabs of reactants have been considered by Leonard and Hill [8] to investigate scalar dissipation and mixing in temporally evolving turbulent reacting flow. The periodic reaction zones (PRZ) model problem described here has two major differences with respect to Leonard and Hill’s problem. The first is that PRZ admits statistically stationary solutions, which are advantageous when studying extinction. The second difference is that PRZ is based on the concept of “anti-flames” to achieve stationary solutions, whereas this is not the case in the temporally evolving case considered by Leonard and Hill.

The velocity field in this model problem is constant-density, statistically stationary, homogeneous isotropic turbulence. At high Reynolds number the velocity field can be characterized by ϵ , the mean dissipation rate and k , the kinetic energy of the turbulence. A mean turbulent frequency $\langle \omega \rangle \equiv \epsilon/k$, and a velocity scale $u' \equiv \sqrt{2k/3}$ are defined in terms of k and ϵ . These quantities can then be used to define a characteristic lengthscale $l = u'^3/\epsilon$ and timescale $\tau = k/\epsilon$ of the turbulence.

The thermochemical state of the fluid is characterized by two composition variables: the mixture fraction $\xi(\mathbf{x}, t)$ and the reaction progress variable $Y(\mathbf{x}, t)$. The mixture fraction is a conserved passive scalar and evolves by

$$\frac{D\xi}{Dt} = \Gamma \nabla^2 \xi, \quad (3)$$

where Γ is the molecular diffusivity. The fluctuating mixture fraction field is defined as

$$\tilde{\xi}(\mathbf{x}, t) = \xi(\mathbf{x}, t) - \langle \xi \rangle(\mathbf{x}, t).$$

In Lee and Pope [7], the mean mixture fraction field is homogeneous, and a statistically homogeneous, periodic, statistically stationary fluctuating mixture fraction field is generated by artificial forcing. In the present work a gradient in the mean mixture fraction field is imposed in the x_2 direction which results in a more realistic “flame brush.” The simplest way to achieve this is to impose a linear gradient $\partial \langle \xi \rangle / \partial x_2 = \text{constant}$. This results in a periodic, statistically

homogeneous fluctuating mixture fraction field, which attains statistical stationarity after sufficient time has evolved for the flow to equilibrate. The mixture fraction variance evolution is given by

$$\frac{\partial \langle \xi^2 \rangle}{\partial t} = -2 \langle \xi u_2 \rangle \frac{\partial \langle \xi \rangle}{\partial x_2} - \langle \chi \rangle, \quad (4)$$

where the terms on the right-hand side are production of mixture fraction variance due to the imposed mean mixture fraction gradient, and mean scalar dissipation

$$\langle \chi \rangle \equiv 2\Gamma \left\langle \frac{\partial \xi}{\partial x_k} \frac{\partial \xi}{\partial x_k} \right\rangle.$$

In stationary isotropic turbulence, the fluctuating mixture fraction field decays in the absence of mean gradient production. The mixing time-scale, which is the characteristic timescale for decay of mixture fraction variance $\xi'^2 = \langle \xi^2 \rangle$, is given by

$$\tau_\phi \equiv \xi'^2 / \langle \chi \rangle. \quad (5)$$

For non-zero values of the imposed linear gradient, the mixture fraction variance attains a stationary value in which there is a balance between production and mean scalar dissipation [9]. It is also found that the pdf of mixture fraction is close to a Gaussian [9].

The reaction progress variable evolution is given by

$$\frac{DY}{Dt} = \Gamma \nabla^2 Y + S(\xi, Y), \quad (6)$$

where $S(\xi, Y)$ is the reaction rate and the molecular diffusivity Γ is taken to be equal to the mixture fraction diffusivity.

A new thermochemical model is employed for a one-step reversible reaction (fuel + oxidant \rightleftharpoons product), which is similar to the one used in Lee and Pope [7]. For the sake of clarity, only the features of the thermochemistry pertinent to this section are presented here. A more complete description is given in Subramaniam and Pope [10]. The reaction progress variable Y is the mass fraction of product. At chemical equilibrium, Y adopts the value $Y_e(\xi)$ which is specified as an analytic expression in terms of ξ and the stoichiometric value of the mixture

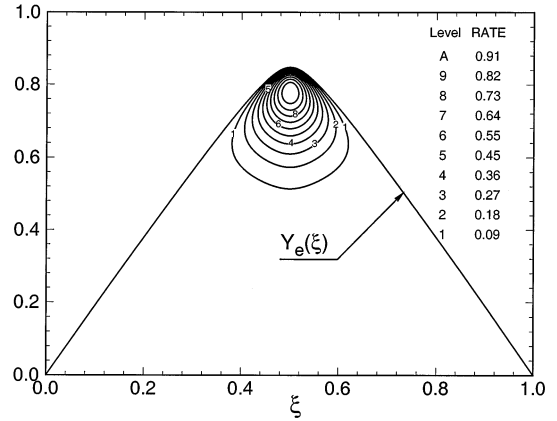


Fig. 1. Sketch of the equilibrium function $Y_e(\xi)$ and normalized reaction rate contours $S(\xi, Y)/S_{\max}$ for the model thermochemistry.

fraction ξ_s ($0 < \xi_s < 1$). The reaction rate is zero at equilibrium [$S(\xi, Y_e) = 0$], and also along the $Y = 0$ contour [$S(\xi, 0) = 0$]. The reaction rate as a function of composition (ξ, Y) is also given by an analytic expression. (The exact specification of these functions and the rationale for developing this thermochemical model is detailed in Subramaniam and Pope [10].) For a stoichiometric mixture fraction of 0.5, Fig. 1 shows a sketch of the equilibrium function and the normalized reaction rate contours.

In combustion problems with two uniform reactant streams, ξ is usually defined as a conserved scalar that goes from zero in one reactant stream (say the oxidant stream) to unity in the second reactant stream (fuel). In this case the mixture fraction everywhere in the flow is bounded by $0 \leq \xi \leq 1$. In contrast to this usual state of affairs, in the periodic reaction zone model problem, ξ is unbounded, and hence the entire thermochemistry requires modified definition and interpretation.

In a DNS of periodic reaction zones, the solution domain is a cube of side L , and a mean gradient of magnitude $\Delta \xi_L / L$ is imposed in the x_2 direction, where the jump in the mean mixture fraction $\Delta \xi_L$ is specified. The velocity $\mathbf{u}(\mathbf{x}, t)$, and the fluctuating component of the mixture fraction $\xi'(\mathbf{x}, t)$ are periodic in all three coordinate directions. The specification of periodic boundary conditions is equivalent to extending the solution domain periodically in all

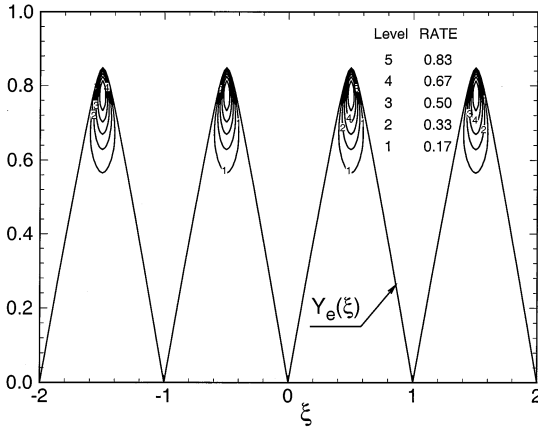


Fig. 2. Symmetric extension of the thermochemistry: equilibrium function and normalized reaction rate contours are shown.

spatial directions. In particular, the periodic boundary condition on ξ implies

$$\xi(x_1, x_2 + mL, x_3, t) = \xi(x_1, x_2, x_3, t), m \text{ integer.}$$

Thus, for the general interval $mL \leq x_2 \leq (m + 1)L$, the mean mixture fraction $\langle \xi \rangle$ ranges from $m\Delta\xi_L$ to $(m + 1)\Delta\xi_L$, and hence for any finite $\Delta\xi_L$, ξ is an unbounded variable over the whole domain. Consequently for this model problem it is necessary to extend the definition of the thermochemistry to all values of ξ . This is done such that

- (i) imposing the periodic boundary condition $[Y(\xi = m) = 0]$ in composition space at the integer-valued mixture fraction isosurfaces $\xi(x, t) = m$, in conjunction with an appropriate extension of $S(\xi, Y)$, results in $Y(x, t)$ periodic in x_2 ,
- (ii) within each interval $[mL, (m + 1)L]$ there is a flame brush, and
- (iii) at sufficiently high Da (far from extinction) Y becomes statistically stationary.

One way to attempt to do this is simply to extend the thermochemistry by periodically repeating the thermochemistry in the $[0, 1]$ mixture fraction interval as depicted in Fig. 2, namely,

$$Y_e(\xi) = Y_e(\xi - \lfloor \xi \rfloor), \quad \xi \notin [0, 1], \quad (7)$$

$$S(\xi, Y) = S(\xi - \lfloor \xi \rfloor, Y), \quad \xi \notin [0, 1], \quad (8)$$

where $\lfloor \xi \rfloor$ is the largest integer smaller than ξ . However, this simple periodic extension is unsuitable since it cannot result in a non-trivial

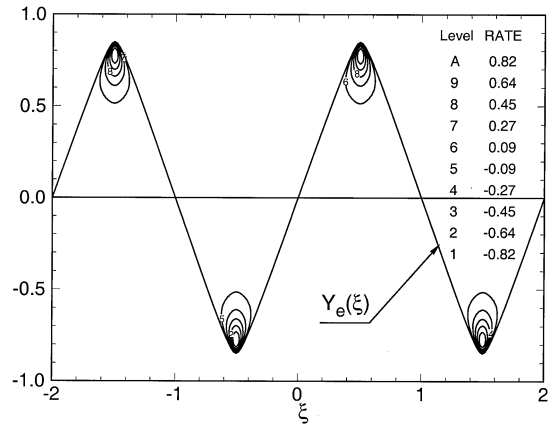


Fig. 3. Antisymmetric extension of the thermochemistry: equilibrium function and normalized reaction rate contours are shown.

stationary solution corresponding to stable reaction [cf. (iii)]. Consider the volume average of the mean progress variable

$$\langle Y \rangle_L(t) \equiv \frac{1}{L} \int_0^L \langle Y \rangle(x_2, t) dx_2.$$

Since in this periodic extension the reaction rate function is always non-negative $[S(\xi, Y) \geq 0]$, the volume average of $\langle Y \rangle$ must always increase (except for the case where the reaction rate is zero everywhere). This implies that there are only two trivial stationary solutions to the problem: either the flow is in chemical equilibrium everywhere ($Y = Y_e$) or there is no product anywhere ($Y = 0$ everywhere). This follows from our assumptions that the reaction rate is zero at equilibrium and along the $Y = 0$ contour. Clearly this extension procedure is not useful for studying the range of combustion phenomena which are of interest.

The alternative extension procedure that is used here is to first extend the thermochemistry in the $[0, 1]$ mixture fraction interval “anti-symmetrically” to the $[-1, 0]$ interval, and then periodically repeat the structure in the mixture fraction interval $[-1, 1]$ as depicted in Fig. 3, specifically

$$Y_e(\xi) = Y_e(\xi - \lfloor \xi \rfloor), \quad \xi \in [2m, 2m + 1], \quad (9)$$

$$Y_e(\xi) = -Y_e(\lfloor \xi \rfloor - \xi), \quad \xi \in [2m - 1, 2m], \quad (10)$$

$$S(\xi, Y) = S(\xi - \lfloor \xi \rfloor, Y), \cdot \xi \in [2m, 2m + 1], \quad (11)$$

$$S(\xi, Y) = -S(\lceil \xi \rceil - \xi, Y), \cdot \xi \in [2m - 1, 2m], \quad (12)$$

where $\lceil \xi \rceil$ is the smallest integer larger than ξ . In order for the mean mixture fraction to extend over one period of the antisymmetric extension of the thermochemistry [i.e., $\langle \xi \rangle(x_2 = 0) = 0$, $\langle \xi \rangle(x_2 = L) = 2$], the jump in the mean mixture fraction over the length L is given by

$$\Delta \xi_L = 2. \quad (13)$$

This implies that the gradient in the mean mixture fraction is $\partial \langle \xi \rangle / \partial x_2 = \Delta \xi_L / L = 2/L$. Since each reaction zone period is statistically identical, it is sufficient to simulate only one such period.

The alternating positive and negative equilibrium functions can be interpreted as zones corresponding to flames and “anti-flames.” In the interval $\xi \in [2m, 2m + 1]$, which is interpreted as a flame, reactants enter from either end of the interval and are converted to product which leaves the interval due to transport. In the interval $\xi \in [2m - 1, 2m]$, which is interpreted as an “anti-flame,” “anti-reactants” (which are products leaving the adjacent flame zones) enter from either end of the interval and are converted to “anti-product” (which is reactant) which again leaves the interval due to transport: see Fig. 3. Each interval in mixture fraction space $\xi \in [2m, 2m + 1]$, is a statistically identical copy of the interval $\xi \in [0, 1]$ and similarly for the “anti-flame” intervals—each interval in mixture fraction space $\xi \in [2m - 1, 2m]$, is a statistically identical copy of the interval $\xi \in [-1, 0]$. Furthermore, each fluid particle in the “anti-flame” interval with composition (ξ, Y) is statistically identical to a fluid particle in the mixture fraction interval $[0, 1]$ with composition $(\lceil \xi \rceil - \xi, -Y)$. As a consequence, even though in this model problem the mixture fraction and progress variable take on seemingly “unphysical” values outside the interval $[0, 1]$, they can be interpreted in physical terms by the mathematical relations in the preceding paragraph.

Flames and anti-flames are separated by the

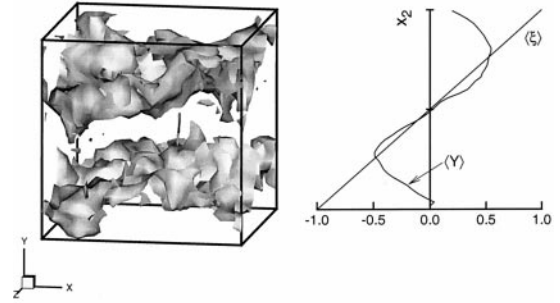


Fig. 4. DNS solution of PRZ with stoichiometric isosurfaces of $\xi = \xi_s = 0.5$ (upper surface) and $\xi = -\xi_s = -0.5$ (lower surface). The corresponding spatial profiles of mean mixture fraction and mean progress variable are shown on the right. Adapted from Overholt and Pope [8] by permission of the authors.

constant-property surfaces, $\xi(\mathbf{x}, t) = \text{integer}$. These surfaces are time-dependent and each one is not necessarily connected. In order to conform with the idea that $\xi = 0$ and $\xi = 1$ correspond to pure reactants (i.e., $Y = 0$), the boundary condition ($Y = 0$) is imposed on the surfaces $\xi = \text{integer}$.

In Fig. 4, the DNS solution of PRZ [11] with isosurfaces of the stoichiometric mixture fraction for the flame and anti-flame is shown. The periodic layered mixture fraction field is clearly visible, with the wrinkled isosurfaces corresponding to fluctuations in the mixture fraction field. The spatial variation of the mean mixture fraction and the mean progress variable in the flow at this time are also shown.

REACTION RATES

The reaction rate function $S(\xi, Y)$, is specified according to the self-similar thermochemical model [10]. The motivation, development and details of this self-similar thermochemistry (SSTC) are described in Subramaniam and Pope [10]. The reaction rate $S(\xi, Y)$ is expressed as

$$S(\xi, Y) = \frac{\Delta \xi_c}{\tau_c} \hat{S}(\hat{\xi}, \hat{y}), \quad (14)$$

where $\Delta \xi_c$ and τ_c are the primary thermochemical parameters, and $\hat{S}(\hat{\xi}, \hat{y})$ is a non-dimensional scaled reaction rate function defined in terms of the scaled variables $\hat{\xi}$ and \hat{y} .

The thermochemical parameter $\Delta\xi_e$ is a mixture fraction scale associated with the curvature of the equilibrium function in mixture fraction space

$$Y_e''(\xi) \equiv d^2 Y_e(\xi)/d\xi^2,$$

and in the SSTC it is defined as

$$\Delta\xi_e \equiv \frac{4}{\pi|Y_{e_{\max}}''|}, \quad (15)$$

where $|Y_{e_{\max}}''|$ is the maximum value of the curvature of the equilibrium function. The other primary thermochemical parameter τ_c , is a chemical timescale which controls the magnitude of the reaction rate, and is varied to simulate different Damköhler numbers.

Now the scaled reaction rate function $\hat{S}(\hat{\xi}, \hat{y})$ is defined. In this study, the stoichiometric value of the mixture fraction ξ_s , is chosen to be 0.5. This results in a symmetric equilibrium function $Y_e(\xi)$. For this symmetric case, the scaled variables $\hat{\xi}$ and \hat{y} in the SSTC are defined as follows:

$$\hat{\xi} = (\xi - \xi_s)/\Delta\xi_e, \quad (16)$$

$$\hat{y} = \frac{Y_e - Y}{\Delta\xi_e}. \quad (17)$$

The scaled reaction rate function $\hat{S}(\hat{\xi}, \hat{y})$ is expressed as a product of two functions,

$$\hat{S}(\hat{\xi}, \hat{y}) = f(\hat{y})g(\hat{\xi}), \quad (18)$$

where,

$$f(\hat{y}) = B\hat{y} \exp(1 - B\hat{y}), \quad (19)$$

$$g(\hat{\xi}) = \exp\{-CG(\hat{\xi})\}, \quad (20)$$

and where $G(\hat{\xi})$ is given by

$$G(\hat{\xi}) \equiv \frac{Y_{\max} - Y_e}{\Delta\xi_e} = \frac{4}{\pi} \hat{\xi} \arctan(\hat{\xi}) - \frac{2}{\pi} \ln[1 + \hat{\xi}^2]. \quad (21)$$

Note that the maximum value of $g(\hat{\xi})$ occurs at $\hat{\xi} = \xi_s$, i.e. $g(0) = 1$. At equilibrium ($y = 0$) f is zero, and it attains its maximum value of 1 at $\hat{y} = B^{-1}$.

The constants B and C are secondary thermochemical parameters that determine the width of the reaction rate function in \hat{y} and $\hat{\xi}$ space, respectively. The parameter B plays the

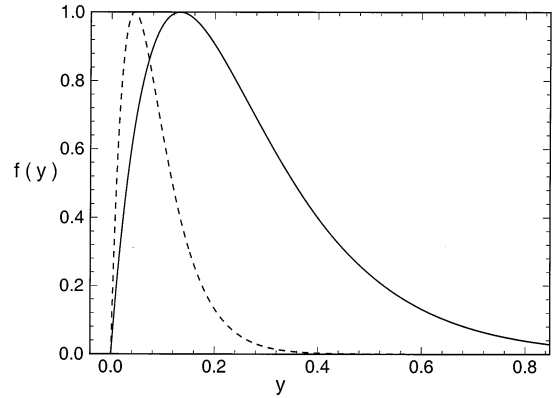


Fig. 5. Plot of the function $f(y)$ showing the reaction zone thickness for the cases that are investigated in the simulations. The self-similar thermochemistry is used with $B = 0.096$. The curves correspond to different values of the parameter $\Delta\xi_e$: — $\Delta\xi_e = 1.27324 \times 10^{-2}$ ($Y_{e_{\max}}'' = -100$), for $\hat{\xi}_r = 10$; - - - $\Delta\xi_e = 4.244 \times 10^{-3}$ ($Y_{e_{\max}}'' = -300$), for $\hat{\xi}_r = 1$ and $\hat{\xi}_r = 0.27$.

role of activation energy. The reaction rate in a typical combustion process is significantly large close to equilibrium and rapidly decays far from equilibrium. This trend is captured by the shape of the function $f(y)$ for suitable choices of the parameter B and $\Delta\xi_e$ (see Fig. 5). The peak of the function g at stoichiometric mixture fraction is also characteristic of the variation of reaction rate in typical combustion systems (see Fig. 6).

Extinction in diffusion flames is often characterized by an S-curve which is a plot of maximum temperature versus a reduced Damköhler number [12]. One way to establish the practical relevance of the present thermochemical model is to demonstrate that the model is capable of reproducing similar extinction characteristics. In Fig. 7 the maximum progress variable (which can be interpreted as temperature) is plotted vs the reciprocal of the normalized mean scalar dissipation rate (equivalent to a Damköhler number normalized by its value at extinction) for simulations performed using this thermochemical model and the conditional moment closure (details of the conditional moment closure are given in the first part of the next section). Similar results were also obtained using the laminar flamelet model. It is clear from Fig. 7 that this thermochemical model reproduces the upper and middle branches of the S-curve which is observed in extinction of diffu-

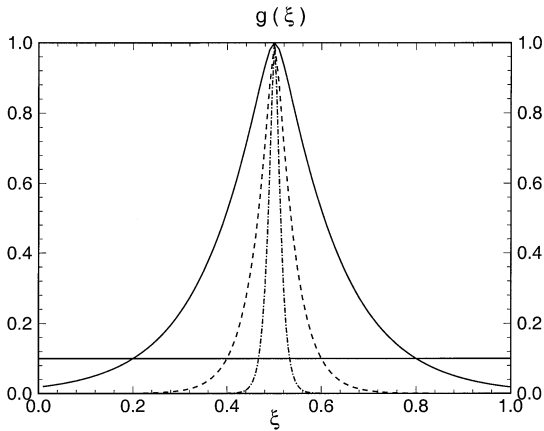


Fig. 6. Plot of the function $g(\xi)$ in the self-similar thermochemistry specification, showing the reaction zone thickness for the three cases that are investigated in the simulations. For $\hat{\xi}_r = 10$ and $\hat{\xi}_r = 1$ the value of C is 0.055, while for $\hat{\xi}_r = 0.27$ it is 0.197. The values of the different reaction zone thickness are: $\Delta\xi_r = 0.6$, $\hat{\xi}_r = 10$; $\Delta\xi_r = 0.2$, $\hat{\xi}_r = 1$; $\Delta\xi_r = 0.067$, $\hat{\xi}_r = 0.27$ (see Table 1). The intersection of the horizontal line at height 0.1 with the function $g(\xi)$ defines the reaction zone thickness $\Delta\xi_r$.

sion flames. The detailed characteristics of the S-curve can be modified by suitable choice of the thermochemical parameters.

The characteristic reaction timescale τ^* associated with this reaction rate specification can be ascertained by considering the Taylor series

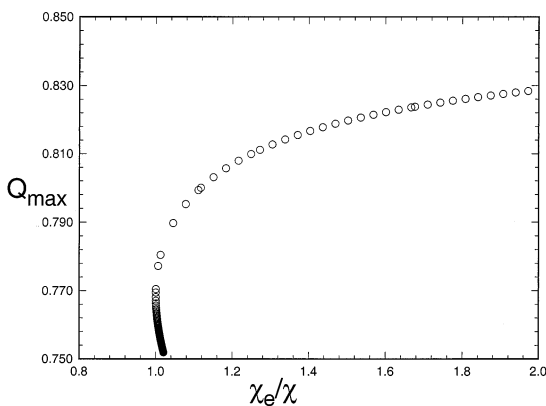


Fig. 7. Extinction characteristics of the thermochemical model represented as the S-curve observed in diffusion flame extinction. The maximum progress variable (temperature) is plotted versus the reciprocal of the normalized mean scalar dissipation rate for simulations performed using the conditional moment closure model. The quantity χ_e represents the mean scalar dissipation rate corresponding to extinction.

expansion of $S(\xi, y)$ in powers of y about the equilibrium contour $y = 0$:

$$S(\xi, y) = S(\xi, 0) + y \left[\frac{\partial S(\xi, y)}{\partial y} \right]_{y=0} + \dots$$

Since $S(\xi, 0)$ is zero (the reaction rate is zero at equilibrium), for small y , the reaction rate is approximately $y[\partial S(\xi, y)/\partial y]_{y=0}$. Noting that

$$\left[\frac{\partial S(\xi, y)}{\partial y} \right]_{y=0} = g(\xi) Be/\tau_c,$$

the reaction rate for small y at $\xi = \xi_s$ (note $g(\xi_s) = 1$) is given by yBe/τ_c . From this relation the characteristic reaction timescale τ^* is deduced to be

$$\tau^* \equiv \tau_c/(Be). \quad (22)$$

At stoichiometric mixture fraction, the reaction rate can be written in terms of the departure from equilibrium y , and the characteristic reaction timescale τ^* as

$$S(\xi_s, y) = \frac{y}{\tau^*} + \mathcal{O}(y^2).$$

It may be noted that the maximum reaction rate is $S_{\max} = \Delta\xi_c/\tau_c = (\Delta\xi_c Be)/\tau^*$. Since both f and g are maximized by unity, τ_c can be used to adjust the actual magnitude of the reaction rate.

The reaction zone thickness in mixture fraction space is defined as

$$\Delta\xi_r = \xi_r - \xi_l, \quad (23)$$

where the lean and rich limits of the reaction zone in mixture-fraction space (ξ_l and ξ_r , respectively) are defined to be the lower and upper values of ξ at which $g(\xi)$ equals 0.1.

Simulations are performed using three different reaction rate specifications corresponding to

TABLE 1

Summary of Thermochemical Parameters for Each Case^a

	$\hat{\xi}_r = 10$	$\hat{\xi}_r = 1$	$\hat{\xi}_r = 0.27$
$\Delta\xi_c$	1.27×10^{-2}	2.24×10^{-3}	2.24×10^{-3}
$ Y''_{e,\max} $	100	300	300
$\Delta\xi_r$	0.6	0.2	0.067
$\Delta\xi_{r,ss}$	0.048	0.016	8.46×10^{-3}
C	0.055	0.055	0.197

^a The thermochemical constant B is 0.096 for all cases.

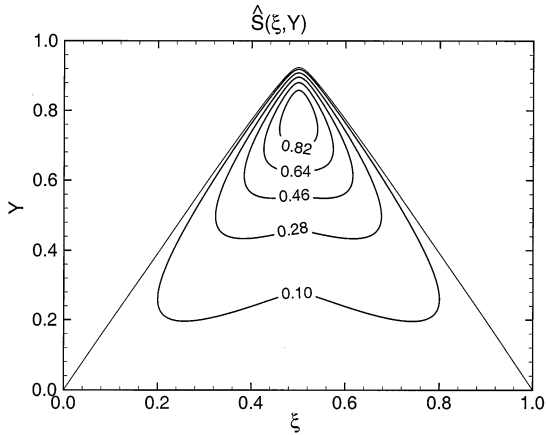


Fig. 8. Contours of the normalized reaction rate function $\hat{S}(\xi, y)$ for the broad reaction zone case: $B = 0.096$, $C = 0.055$.

broad ($\hat{\xi}_r \equiv \Delta\xi_r/\xi' = 10$), moderate ($\hat{\xi}_r = 1$) and thin ($\hat{\xi}_r = 0.27$) reaction zones. The values of the thermochemical parameters (barring the chemical timescale τ_c) used in these three cases are tabulated in Table 1. The corresponding functions $f(y)$ and $g(\xi)$ are shown in Figs. 5 and 6, respectively. The normalized reaction rate functions for the broad, moderate and thin reaction zone cases are shown in Figs. 8–10, respectively. For simulations with the same reaction zone thickness, when the value of τ_c is varied (in order to simulate different Damköhler numbers) there is a corresponding change in the magnitude of the reaction rate. However, the shape of the reaction rate func-

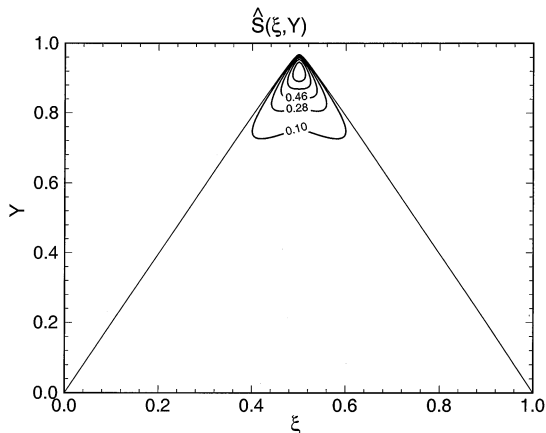


Fig. 9. Contours of the normalized reaction rate function $\hat{S}(\xi, y)$ for the moderate reaction zone case: $B = 0.096$, $C = 0.055$.

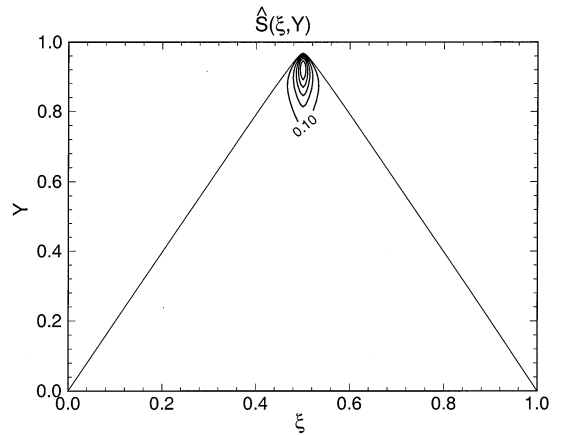


Fig. 10. Contours of the normalized reaction rate function $\hat{S}(\xi, y)$ for the thin reaction zone case: $B = 0.096$, $C = 0.197$.

tion in composition space remains the same for all simulations with the same reaction zone thickness. The rationale for choosing these particular values of the thermochemical parameters may be found in Subramaniam and Pope [10].

TURBULENT COMBUSTION MODELS

Conditional Moment Closure

In this section the conditional moment closure (CMC) model of Bilger [13], as applied to the periodic reaction zone problem, is described. The starting point for the derivation of the CMC model equation is the evolution of the mixture-fraction and progress variable fields (Eqs. 3, 6). In a turbulent flow, both $Y(\mathbf{x}, t)$ and $\xi(\mathbf{x}, t)$ are random fields. The sample space variable of ξ is denoted by η . The expectation of $Y(\mathbf{x}, t)$ conditional on $\xi(\mathbf{x}, t) = \eta$ is denoted $Q(\eta, \mathbf{x}, t)$, i.e.,

$$Q(\eta, \mathbf{x}, t) \equiv \langle Y(\mathbf{x}, t) | \xi(\mathbf{x}, t) = \eta \rangle. \quad (24)$$

For brevity $\langle Y(\mathbf{x}, t) | \xi(\mathbf{x}, t) = \eta \rangle$ is denoted by $\langle Y | \eta \rangle$. The deviation $\tilde{y}(\mathbf{x}, t)$ of the progress variable $Y(\mathbf{x}, t)$ from its conditional mean is defined as

$$\tilde{y}(\mathbf{x}, t) = Y(\mathbf{x}, t) - Q(\xi[\mathbf{x}, t], \mathbf{x}, t). \quad (25)$$

The evolution equation for $Q(\eta, \mathbf{x}, t)$ is

$$\frac{\partial Q}{\partial t} + \langle U_i | \eta \rangle \frac{\partial Q}{\partial x_i} = S(\eta, Q) + \Gamma \langle \nabla \xi \cdot \nabla \xi | \eta \rangle \frac{\partial^2 Q}{\partial \eta^2} + e_Q + e_{\bar{y}}, \quad (26)$$

where

$$e_Q = \Gamma \left[\frac{\partial}{\partial x_i} \left(\frac{\partial Q}{\partial x_i} \right) + \frac{\partial^2 Q}{\partial \eta \partial x_i} \left\langle \frac{\partial \xi}{\partial x_i} \middle| \eta \right\rangle \right] \quad (27)$$

and

$$e_{\bar{y}} = - \left\langle \left(\frac{\partial \bar{y}}{\partial t} + U_i \frac{\partial \bar{y}}{\partial x_i} - \Gamma \frac{\partial^2 \bar{y}}{\partial x_i \partial x_i} \right) \middle| \eta \right\rangle. \quad (28)$$

Consistent with the basic assumption that the difference between $Y(x, t)$ and its mean conditioned on the mixture fraction is small, the terms in $e_{\bar{y}}$ are assumed to be negligible compared to the other terms in the equation for Q . At sufficiently high Reynolds number, the terms in e_Q are also negligible [13].

If fluctuations in Y arise from fluctuations in ξ and if the fluctuating mixture fraction field is statistically homogeneous, then $\partial Q / \partial x_i$ must be negligible. By using these closure hypotheses, Eq. (26) can be written as

$$\frac{\partial Q}{\partial t} = S(\eta, Q) + \frac{\langle \chi | \eta \rangle}{2} \frac{\partial^2 Q}{\partial \eta^2}, \quad (29)$$

where $\chi = 2\Gamma \nabla \xi \cdot \nabla \xi$ is defined to be the scalar dissipation. The conditional mean scalar dissipation, $\langle \chi | \eta \rangle$ is assumed to be equal to the unconditional mean scalar dissipation $\langle \chi \rangle$ since the pdf of ξ is Gaussian. For stationary solutions the temporal derivative must be zero, and the resulting final form of the equation for Q is

$$\frac{\partial^2 Q}{\partial \eta^2} + \frac{2S(\eta, Q)}{\langle \chi \rangle} = 0. \quad (30)$$

The boundary conditions on Q are $Q(\eta = 0) = 0$ and $Q(\eta = 1) = 0$.

The reaction rate expression corresponding to the self-similar thermochemistry (Eqs. 14 and 18) can be substituted into Eq. 30 to obtain

$$\frac{\partial^2 Q}{\partial \eta^2} + \frac{2}{\langle \chi \rangle} \frac{\Delta \xi_e f(\hat{q}) g(\hat{\eta})}{\tau_c} = 0, \quad (31)$$

where $\hat{q} = q / \Delta \xi_e$, $q = Y_c(\eta) - Q(\eta)$, and $\hat{\eta} = (\eta - \xi_s) / \Delta \xi_e$. Substituting the expression for the

mixing timescale in terms of the scalar dissipation (Eq. 5) and the expressions for the functions f and g (Eqs. 19 and 20) in Eq. 31 results in

$$\frac{\partial^2 Q}{\partial \eta^2} + \frac{2}{\xi'^2} \Delta \xi_e \hat{q} \exp\{[-B\hat{q} - CG(\hat{\eta})]\} \cdot \frac{\tau_\phi B e}{\tau_c} = 0. \quad (32)$$

The CMC equation (Eq. 32) can be rewritten in terms of the non-dimensional parameters Da and $\hat{\xi}_{r_{ss}}$ by using the relations in Eqs. 22 and 1 as

$$\frac{\partial^2 Q}{\partial \eta^2} + \frac{1}{\Delta \xi_e} \hat{q} \exp\{[-B\hat{q} - CG(\hat{\eta})]\} \cdot Da \hat{\xi}_{r_{ss}}^2 \left(\frac{8C}{\pi} \right) = 0, \quad (33)$$

where $\Delta \xi_{r_{ss}} \equiv \Delta \xi_e \sqrt{\pi / (4C)}$, and $\hat{\xi}_{r_{ss}} = \Delta \xi_{r_{ss}} / \xi'$. This equation admits stable solutions only for a limited range of parameter values Da and $\hat{\xi}_{r_{ss}}$. For given $\hat{\xi}_{r_{ss}}$, there is a critical value of Da , $Da_{crit}(\hat{\xi}_{r_{ss}})$, below which Eq. 33 admits no solutions, while for Da greater than Da_{crit} there are two solutions: one of which is stable and the other which is unstable. By solving for the critical Damköhler number corresponding to the desired range of values in $\hat{\xi}_{r_{ss}}$ space (while keeping the thermochemical constants B and C fixed), the global extinction boundary as predicted by the CMC model can be determined in $Da - \hat{\xi}_{r_{ss}}$ space.

PDF Method

In Monte Carlo simulations of inhomogeneous flows the solution domain in physical space is discretized into a number of cells for the purpose of extracting local mean quantities that appear in the particle evolution equations. Within each cell at any given time t , the joint pdf of velocity, composition and turbulent frequency is represented by an ensemble of N particles. The position, velocity and turbulent frequency of the i th particle are denoted by $\mathbf{X}^{(i)}$, $\mathbf{U}^{(i)}$ and $\omega^{(i)}$ respectively. If the number of compositions is D , then $\phi_{\beta i}$ ($\beta = 1, \dots, D$) represents the composition of the i th particle ($i = 1, \dots, N$). Each particle is assigned an

importance weight w_i (such that the particle weights sum to unity) which determines its relative contribution in estimates of the means and higher order moments of the particle properties.

Physical Sub-models

The evolution equations of the particle properties are:

$$d\mathbf{X}^{(i)} = \mathbf{U}^{(i)} dt \quad (34)$$

$$d\mathbf{U}^{(i)} = -\frac{3}{4} C_0 \langle \omega \rangle (\mathbf{U}^{(i)}(t) - \langle \mathbf{U} \rangle) dt + \sqrt{C_0 k \langle \omega \rangle} d\mathbf{W} \quad (35)$$

$$d\omega^{(i)} = -(\omega^{(i)} - \langle \omega \rangle) C_3 \langle \omega \rangle dt - \langle \omega \rangle \omega^{(i)} S_\omega dt + \sqrt{\{2\sigma^2 \langle \omega \rangle \omega^{(i)} C_3 \langle \omega \rangle\}} dW^* \quad (36)$$

$$\frac{d\phi_{\beta i}}{dt} = \Theta_\beta^{(i)} + S_\beta([\phi_i]), \quad \beta = 1, 2. \quad (37)$$

The position equation simply states that each particle moves with its own velocity. The mean quantities in Eqs. 35 and 36 are evaluated at $(\mathbf{X}^{(i)}, t)$. The velocity evolves by the simplified Langevin model for *stationary* isotropic turbulence with the constant-density simplification [14], [15]. The model constant C_0 is fixed at its standard value of 2.1. The term $d\mathbf{W}$ represents an increment in the isotropic Wiener process $\mathbf{W}(t)$. The details of this model and its performance may be found in Pope [16]. The turbulent frequency evolves by the Jayesh and Pope [17] model with simplifications resulting from the homogeneity assumption incorporated in Eq. 36. In the equation for turbulent frequency (Eq. 36), the term dW^* represents an increment in the Wiener process $W^*(t)$, which is independent of the Wiener process in the velocity equation. For stationary homogeneous turbulence the modeled source term S_ω is set to zero, thus ensuring that $\langle \omega \rangle$ is stationary. The values of the model constants in the turbulent frequency equation are $C_3 = 1$ and $C_4 = 0.25$. The pdf of the stationary and homogeneous turbulent frequency is a gamma distribution. Further details of the turbulent frequency model may be found in Jayesh and Pope [17]. The composition variables are defined as $\phi_1 = \xi$

and $\phi_2 = Y$. In the composition evolution equation (Eq. 37), the term Θ_β represents the mixing model, the term $S_\beta([\phi_i])$ represents the reaction rate of the β th scalar (which is non-zero only for $\beta = 2$), and $[\phi_i]$ represents the vector of compositions corresponding to the location of the i th particle in composition space. The self-similar model thermochemistry specification for the reaction rate is used. The two different mixing models used in this study, IEM and EMST, are now described.

Mixing Models

A comprehensive discussion of the issues concerning pdf mixing models may be found in Subramaniam and Pope [5]. It is shown in that work that mixing models should satisfy several performance criteria including the properties of boundedness, independence, and extension to multiple reactive scalars. Current mixing models reflect a compromise between these various performance criteria since none of them satisfies all the criteria. In the context of modeling nonpremixed turbulent reacting flows, it is our belief that the properties of boundedness, extension to multiple scalars, and localness in composition space, are the most important performance criteria. Consequently some pdf mixing models have not been considered in this study in spite of their excellent performance with respect to some of the other performance criteria. Notable among those omitted are the mapping closure mixing model [18, 19], and the binomial Langevin model [20]. The mapping closure model is omitted in spite of its excellent performance in the decaying scalar test because for multiple scalars the mappings become non-unique, and the model is dependent on the species ordering that is chosen. Similarly, even though the binomial Langevin model performs very well in the decaying scalar test, it is not considered in this study since the imposition of boundedness in the multiple scalar case introduces a dependency of the model results on species order.

One of the salient conclusions in Subramaniam and Pope [5] is that mixing models should be local in composition space, in order to accurately model the physics of mixing in nonpremixed turbulent reacting flows. This modeling

principle is not incorporated in mixing models such as the IEM [21], Curl's [22], and modified Curl's model. The IEM model is chosen as representative of this family of models that are non-local in composition space. In Subramaniam and Pope [5] it was shown that the IEM model performs poorly in the diffusion flame test problem, since it is non-local in composition space. Norris and Pope [23] have also shown that both Curl's and modified Curl's model also perform poorly in the diffusion flame test for the same reason.

In the IEM model [21], the i th particle's compositions evolve by

$$\frac{d\phi_{\beta i}}{dt} = -\frac{1}{2} C_{\phi} \langle \omega \rangle (\phi_{\beta i} - \langle \phi_{\beta} \rangle), \quad (38)$$

where C_{ϕ} is a model constant chosen to be 2.0. While this model is attractive on account of its simplicity it is known to perform unsatisfactorily in certain reactive flows [23, 4].

The EMST mixing model is based on interactions between particles that are local in composition space. It is an extension of the mapping closure particle model to multiple scalars. Only the salient features of the model are presented here for completeness. A complete description of the EMST model and its validation in inert and reactive tests may be found in Subramaniam and Pope [5] and [6].

At any given time a subset of N_T particles is chosen for mixing from the ensemble of N particles in the cell, based on an age property associated with each particle. A Euclidean minimum spanning tree is constructed on this subset of N_T particles so that each particle is connected with at least one neighbor particle (see Fig. 11). The vector of particle compositions $\phi_{(i)} = \phi_{\beta(i)}$, $i = 1, \dots, N_T$ evolves as

$$w_{(i)} \frac{d\phi_{(i)}}{dt} = -\alpha \sum_{\nu=1}^{N_T-1} B_{\nu} \{ (\phi_{(i)} - \phi_{n_{\nu}}) \delta_{im_{\nu}} + (\phi_{(i)} - \phi_{m_{\nu}}) \delta_{in_{\nu}} \}, \quad (39)$$

where the ν th edge connects the particle pair (m_{ν}, n_{ν}) and δ represents the Kronecker delta. The specification of the model constants B_{ν} and α is described in Subramaniam and Pope [5], and [6].

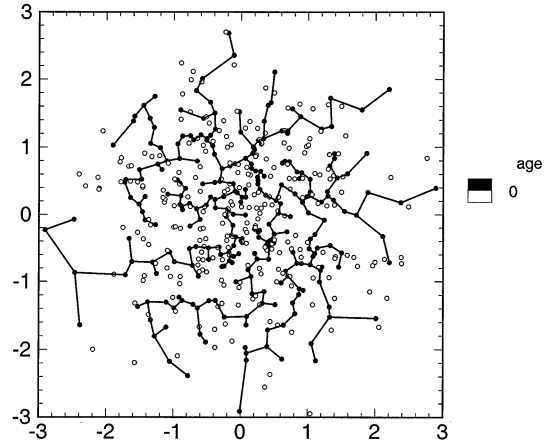


Fig. 11. Euclidean Minimum Spanning Tree constructed on the mixing subset of an ensemble of particles in 2-D composition space (open circles represent particles in the non-mixing state); $N = 512$ particles, joint-normal distribution.

The PDF2DV Program

These physical sub-models are incorporated in a FORTRAN program called PDF2DV developed by Pope [24] to calculate the properties of statistically two-dimensional (plane or axis-symmetric) turbulent reactive flows. The problem under consideration has spatial structure in only the x_2 direction. Periodic boundary conditions are imposed at $x_2 = 0$ and $x_2 = L$ on the fluctuating velocity, turbulent frequency, fluctuating mixture fraction and progress variable. The flow parameters for the simulations are given in Tables 2 and 3.

The grid is chosen to be uniform in the computational domain $0 \leq x_2 \leq L$ and the grid spacing is chosen such that there are at least five computational cells per integral scale l (see Table 4). Only the mean progress variable field $\langle Y(\mathbf{x}, t) \rangle$ has a spatial variation in x_2 that has to

TABLE 2

Summary of Velocity-Field Statistics Which are Common to all the Cases in the PDF Simulations

l —integral length scale	1.0
k —turbulent kinetic energy	1.5
u' —turbulence intensity ($\sqrt{2k/3}$)	1.0
ϵ —mean dissipation rate	1.0
$\langle \omega \rangle$ —mean turbulent frequency (ϵ/k)	0.67
τ —turbulence timescale	1.5
τ_{ϕ} —mixing timescale	0.75

TABLE 3

Summary of Case-Specific Flow Parameters in the PDF Simulations

	$\xi_r = 10 \quad \xi_r = 1 \quad \xi_r = 0.27$		
L —computational box-length	31.13	9.34	7.78
ξ' —nominal r.m.s. mixture fraction	0.06	0.2	0.24
T_t —transport timescale	58.1	5.23	3.63

be resolved. This is guaranteed provided the fluctuating mixture fraction field (i.e., the flame brush) is resolved spatially.

In the periodic reaction zones problem the mixture fraction variance attains a stationary value when the production due to mean gradient balances the scalar dissipation. The r.m.s. value of the stationary mixture fraction scales as

$$\xi' \sim \frac{\partial \langle \xi \rangle}{\partial x_2} \times l. \quad (40)$$

If the length of the computational domain in the x_2 direction is L and $\Delta \xi_L$ is the jump in mean mixture fraction across the domain, then substituting

$$\frac{\partial \langle \xi \rangle}{\partial x_2} = \frac{\Delta \xi_L}{L},$$

the r.m.s. mixture fraction scaling can be written as

$$\xi' \sim \Delta \xi_L \frac{l}{L}. \quad (41)$$

Using this relation between the r.m.s. mixture fraction ξ' and the integral scale l (Eq. 41), it is clear that resolving the integral scale l ensures that all the composition mean fields are spatially well resolved.

Particle properties are advanced over a time

step Δt , chosen such that all important flow timescales are resolved (see Table 4), using the method of fractional steps [14]. The time step restriction on Δt arises from the convective timescale which is the smallest of the flow timescales. The effects of mixing and reaction on the reactive scalar Y are implemented through a first-order splitting strategy [25]. The change in Y due to reaction over a time step Δt is computed analytically (details in [6], [10]), thus avoiding the need for expensive sub-stepping of the chemical timescale which would have made the high Damköhler number calculations prohibitive. The particle number density is uniform in physical space. For small values of $\hat{\xi}_r$, within a computational cell, the thermochemical composition scales ($\Delta \xi_r$ and $\Delta \xi_c$) are a small fraction of the region accessed by the particle compositions (which is determined by the r.m.s. mixture fraction ξ'). For these cases, the number of particles per cell N_{pc} has to be increased to ensure that the thermochemical scales are adequately resolved. For the details of the convergence of important flow statistics with respect to N_{pc} the reader is referred to Subramaniam [6], [10].

DESCRIPTION OF TEST CASES

The turbulent velocity field parameters which are the same for all the cases are tabulated in Table 2. The different value of stationary mixture fraction standard deviation for each case is generated by changing L , the length of the computational domain. Since the jump in the mean mixture fraction over the computational box-length L is held fixed at 2, changing L effectively changes the imposed mean mixture fraction gradient. The different computational

TABLE 4

Summary of Numerical Parameters for Each Case in the PDF Simulations

	$\hat{\xi}_r = 10$	$\hat{\xi}_r = 1$	$\hat{\xi}_r = 0.27$
N_c —number of cells in $[0, L]$	156	50	40
$\Delta x_2/l$ —spatial resolution	0.2	0.19	0.19
N_{pc} —nominal number of particles per cell:	80	750	1120
$C_{\Delta t_m} \Delta t \leq C_{\Delta t_m} \tau_\phi$	0.1	0.1	0.1
$C_{\Delta t_u} \Delta t \leq C_{\Delta t_u} \Delta x_2 / (2u')$	0.4	0.4	0.4
Δt —time step	0.036	0.036	0.038

box-lengths, mixture fraction standard deviation and associated transport timescale are tabulated in Table 3. The fundamental and derived thermochemical parameters for each case are given in Table 1.

The case with $\hat{\xi}_r = 10$ ($\xi' \approx 0.06$, $\Delta\xi_r = 0.6$) corresponds to broad reaction zones. Consider fluid at a physical location where the mean mixture fraction is stoichiometric. The fluctuations in mixture fraction at this location are small compared to $\Delta\xi_r$ and are almost always confined within the reaction zone in composition space. The case with $\hat{\xi}_r = 1$ ($\xi' \approx 0.2$, $\Delta\xi_r = 0.2$) corresponds to moderate reaction zone thickness parameter. The mixture fraction fluctuations are of the order of the reaction zone thickness $\Delta\xi_r$. The case with $\hat{\xi}_r = 0.27$ ($\xi' \approx 0.24$, $\Delta\xi_r = 0.067$) corresponds to thin reaction zones. The mixture fraction fluctuations are large compared to the reaction zone thickness $\Delta\xi_r$. This is expected to be a severe test of the mixing models.

Simulation Strategy

The objective is to perform simulations for each of the three cases (corresponding to fixed values of $\hat{\xi}_r$) for a range of Damköhler numbers spanning the range of physical states from stable reaction to global extinction. One important outcome of these simulations will be an estimate of the critical Damköhler corresponding to global extinction.

In order to obtain these estimates it is necessary to quantitatively characterize global extinction in a PDF simulation. In the DNS of homogeneous combustion Lee and Pope [7] used an imbalance index, which is a non-dimensional measure of the imbalance between mixing and reaction terms in the evolution equation of the volume-averaged-perturbation $[y(x, t)]$ [7], to characterize global extinction. In the present study an extinction index is defined based on the temporal evolution of the particle composition values in the PDF simulation.

Extinction Index

All the simulations are evolved from the initial condition of chemical equilibrium. In composition space all the particles initially lie along the

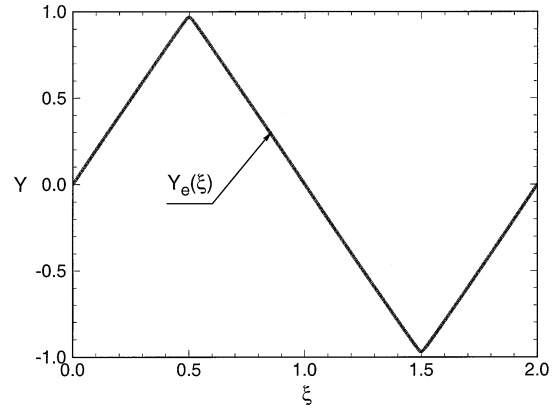


Fig. 12. Initial condition for the PDF simulations: mixture fraction ξ is uniformly distributed in $[0, 2]$; progress variable Y is initially at equilibrium $Y_e(\xi)$.

equilibrium line $Y_e(\xi)$. See Figure 12. After sufficient time has elapsed for the effect of initial conditions to be negligible, the particle properties reach statistical stationarity.

At very high Da , reaction forces these particles to remain close to the equilibrium line, while mixing tends to draw them away from equilibrium. At the other extreme if there is no reaction (inert case), then mixing forces the particles to the $Y = 0$ line, which corresponds to global extinction. Intermediate values of the Da number result in particles populating the composition plane somewhere between these two extreme states. At any time t , one measure of the departure of particles from the equilibrium line in composition space is the expectation of the progress variable conditioned on mixture fraction $\langle Y|\xi \rangle(t)$. However, it is preferable to characterize extinction by a single variable rather than a function. An alternative measure could be the mean progress variable evaluated at the physical location where the mean mixture fraction is stoichiometric, $[\langle Y \rangle(x_2, t)]_{\langle \xi \rangle(x_2) = \xi_s}$. This physical location is always at $x_2 = L/4$ in the simulations and the mean progress variable at this location is denoted $\langle Y \rangle_s(t) \equiv \langle Y \rangle(L/4, t) = [\langle Y \rangle(x_2, t)]_{\langle \xi \rangle(x_2) = \xi_s}$.

However, this measure suffers from two drawbacks. Firstly, it is subject to relatively large statistical variations (since only the particles in the cell located at $x_2 = L/4$ contribute to this quantity) and secondly for the broad reaction zones case this quantity is not truly representa-

tive of the state of particles in the reaction zone. To alleviate both these difficulties, instead of using $\langle Y \rangle_s$ it is preferable to use the reaction-zone-conditioned mean progress variable $\langle Y | \xi_R \rangle$. For $0 \leq \xi \leq 1$ this is defined as

$$\langle Y | \xi_R \rangle \equiv \langle Y^{(i)} | \xi_1 \leq \xi^{(i)} \leq \xi_r \rangle. \quad (42)$$

This quantity is a direct measure of the state of particles in the reaction zone.

Furthermore, noting that each fluid particle in the “anti-flame” interval with composition (ξ, Y) is statistically identical to a fluid particle in the mixture fraction interval $[0, 1]$ with composition $([\xi] - \xi, -Y)$, the particle composition values ($|Y^{(i)}|$) in the “anti-reaction zone” may be used in computing $\langle Y | \xi_R \rangle$, thereby reducing the statistical error.

For the inert case, the decay of the mean progress variable can be estimated. Once stationarity is reached, the ratio of the change in $\langle Y | \xi_R \rangle(t)$ from its value at $t = T_t$ (T_t is the transport timescale defined below) to the change in $\langle Y | \xi_R \rangle(t)$ from its value at $t = T_t$ for the decaying inert case can be used to quantify extinction.

If the characteristic lengthscale of variation of $\langle Y \rangle$ in x_2 is L , and $\langle u_2 Y \rangle$ is estimated using the standard eddy diffusivity approximation as $\langle u_2 Y \rangle \sim \gamma_t \partial \langle Y \rangle / \partial x_2$, then to a good first approximation:

$$\langle Y \rangle(x_2, t) = \langle Y \rangle(x_2, 0) \exp(-t/T_t),$$

where the transport timescale $T_t = L^2/\gamma_t$. Numerical simulations confirm this behavior with $T_t \approx 0.04 (L/l)^2 \tau$.

Using $\langle Y | \xi_R \rangle$ the extinction index $[E.I.(t)]$ is defined as

$$E.I.(t) \equiv \frac{[\langle Y | \xi_R \rangle(t) - \langle Y | \xi_R \rangle(T_t)]}{[\langle Y | \xi_R \rangle(T_t)(\exp(1 - t/T_t) - 1)]}, \quad t > T_t. \quad (43)$$

The denominator is the change in $\langle Y | \xi_R \rangle$ from $t = T_t$ if the flow were inert, and the numerator is the corresponding change in $\langle Y | \xi_R \rangle$ for non-zero reaction at the Damköhler specified in the simulation. The changes in $\langle Y | \xi_R \rangle$ are computed with respect to the $t = T_t$ instant so as to ensure that the effect of initial conditions is negligible by $t = T_t$, the largest timescale in the flow.

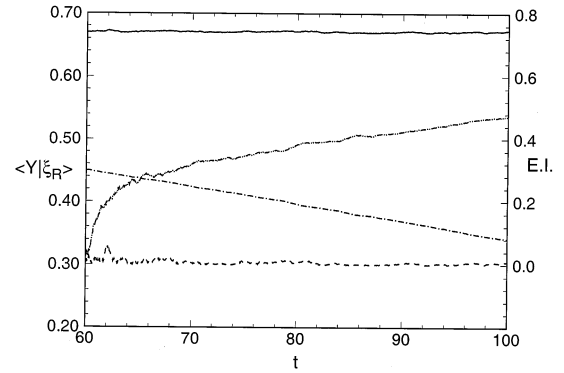


Fig. 13. Evolution of $\langle Y | \xi_R \rangle$ and $E.I.$ for the $\hat{\xi}_r = 10$ case. $Da = 5$ (stable reaction): — $\langle Y | \xi_R \rangle$, - - - $E.I.$; $Da = 0.35$ (extinction): - · - · $\langle Y | \xi_R \rangle$, · · · $E.I.$

Given the statistical variability inherent in turbulent flows, global extinction can only be quantified probabilistically. In Lee and Pope [7] the authors suggest two possible ways to quantify global extinction: (i) the probability of extinction at a normalized time and (ii) the normalized mean time to extinction in the context of DNS. Both these quantities are beyond the scope of current computational capabilities for either PDF or DNS. In this light, an imprecise definition of extinction for practical purposes is used based on the extinction index. At any Da^* , after the simulation has evolved for a time T_s (where $T_s > T_t$ and is usually two to four times T_t)

if $E.I.(T_s) \geq 0.25$: global extinction \forall

$$Da \leq Da^*,$$

else if $E.I.(T_s) < 0.25$: stable reaction \forall

$$Da \geq Da^*.$$

The evolution of the extinction index for representative cases showing stable reaction and extinction is presented in Fig. 13. By performing simulations for a range of Da , starting from a very high value of Da which is evolved for $T_s \sim [2 - 4]T_t$ and then progressively reducing the Da in steps by a fixed fraction (and evolving the flow for T_s at each Da), a rough bracket of the critical Damköhler number $[Da_l, Da_u]$ corresponding to global extinction can be determined using the criterion expressed in Eq. 43. This then implies that for $Da > Da_u$ there is stable

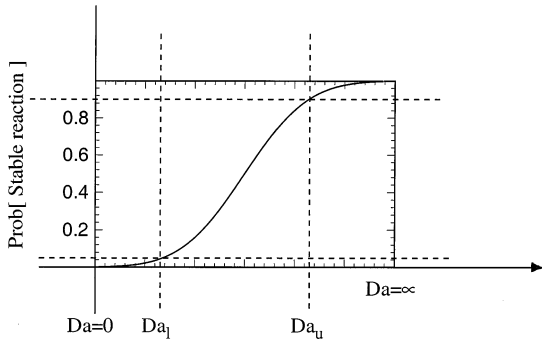


Fig. 14. Sketch of the probability of stable combustion showing plausible locations for the lower and upper brackets on the critical Damköhler number.

reaction with high probability and that for $Da < Da_l$ there is a high probability of global extinction. A sketch of the variation of probability of stable reaction with Damköhler is shown in Fig. 14.

Simulation Algorithm

The simulations and the prediction of global extinction based on *E.I.* are sensitive to the initial condition from which the run is started and are also subject to statistical variability. The effect of statistical variability can be quantified, within the bounds of the computational expense-accuracy trade-off, by performing multiple independent simulations (MIS) at a given Damköhler number. Thus by performing say M MIS at Da_u and Da_l , the probability of extinction (or stable reaction) can be estimated at Da_l and Da_u .

The sensitivity to initial conditions requires that the ratio by which the Damköhler is reduced in the search for $[Da_l, Da_u]$ not be so large as to cause extinction when a smaller ratio would have led to stable reaction. An acceptable value for this ratio is determined empirically to be 0.7.

The considerations of statistical variability and sensitivity to initial conditions dictate the formulation of the following simulation algorithm, which enables extracting the $[Da_l, Da_u]$ estimates from the simulations accurately, at minimum computational cost.

Algorithm:

0. Establish stable reaction at a high Damköhler denoted Da_0 (estimated from

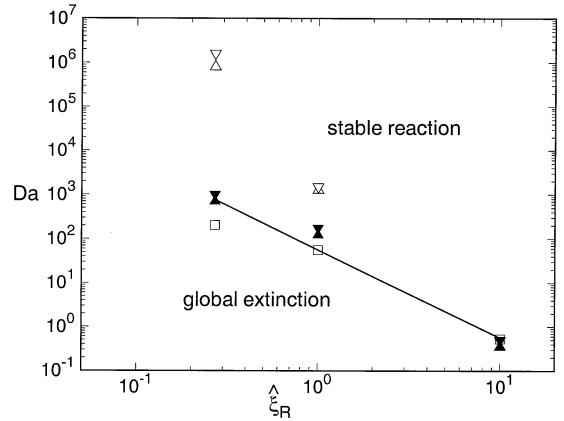


Fig. 15. Stability diagram in the $Da-\xi_r$ plane showing the different model predictions for the stability boundary: \square CMC; open triangles IEM; solid triangles EMST. The line represents $Da = 56.02 \xi_r^{-2}$.

the CMC predictions) by evolving the flow for $T_s = 3T_t$.

1. Reduce the Damköhler by a pre-determined factor (0.5) in a series of steps, evolving each Da for $T_s = 2.1T_t$ till global extinction is observed. Thus obtain preliminary estimates for $[Da_l, Da_u]$.
2. Perform multiple ($M = 4$) independent simulations¹ starting at the preliminary estimate Da_u , reducing the Da by a factor of 0.7, evolving the flow for $T_s = 3T_t$ or to extinction, whichever is earlier. Thus obtain refined estimates of $[Da_l, Da_u]$ and estimates of the probability of extinction at these Damköhler numbers.

Results

The model predictions for the stability limits in $Da-\xi_r$ space are shown in Fig. 15. See Table 5. The CMC model predictions for the critical Damköhler corresponding to extinction scale as ξ_r^{-2} for the $\xi_r = 10$ and $\xi_r = 1$ cases, as expected. The prediction for the thin reaction zone case ($\xi_r = 0.27$) deviates from this scaling since the thermochemical constant C is different for this case. While there is reasonably good agreement

¹ For the $\xi_r = 0.27$ case the IEM model prediction for critical Damköhler number differs from the CMC and EMST predictions by several orders of magnitude. Multiple independent simulations were not performed for this case since the IEM model is grossly in error.

TABLE 5

Global Extinction Predictions

	$\hat{\xi}_r = 10$	$\hat{\xi}_r = 1$	$\hat{\xi}_r = 0.27$
Da_{crit} (CMC)	0.527	56.02	204.2
$[Da_1, Da_u]$ (IEM)	[0.35, 0.5]	[1260, 1500]	$[8 \times 10^5, 1.6 \times 10^6]$
$[Da_1, Da_u]$ (EMST)	[0.35, 0.5]	[122.5, 175]	[700, 1000]

among the models for broad reaction zones, it is found that the predictions diverge with decreasing reaction zone thickness parameter. The definition of global extinction used in this study is largely insensitive to the effect of statistical variability. For the cases where MIS were performed (the only exception being the IEM for $\hat{\xi}_r = 0.27$ for reasons noted earlier), it is found that all four simulations exhibited stable combustion at Da_u and global extinction at Da_1 . However, these results must be cautiously interpreted within the limited definition of global extinction used in this study.

Quantitative comparisons of the model predictions are also made and the statistic that is compared is defined in terms of the mean perturbation from equilibrium of the progress variable conditioned on the reaction zone $\langle y|\xi_R \rangle(t)$, which is defined as

$$\langle y|\xi_R \rangle(t) \equiv \langle (Y_e(\xi^{(i)}(t)) - Y^{(i)}(t)) \rangle$$

$$\xi_l \leq \xi^{(i)}(t) \leq \xi_r. \quad (44)$$

This quantity attains a stationary state after one transport timescale T_t has elapsed and time-averaging may be performed for $t > T_t$. The predictions of the PDF models for this time-averaged quantity, $[\langle y|\xi_R \rangle]_T$ are compared with the average value of $q(\eta)$ in the reaction zone obtained from the CMC predictions in Table 6. The results are now discussed on a case-by-case basis.

Broad Reaction Zone Case: $\hat{\xi}_r = 10$

For this case the numerical parameters used to obtain the CMC result are tabulated in Table 7. The CMC model prediction for the critical Damköhler number for $\hat{\xi}_r = 10$ is 0.527. The perturbation of the conditional mean progress variable from equilibrium (q_M) at Da_{crit} is shown in Fig. 16. The IEM prediction for this case is ($Da_1 = 0.35$, $Da_u = 0.5$). The scatter

plots for $Da = 0.5$ and $Da = 0.35$ are shown in Figs. 17 and 18, respectively. The EMST prediction for this case is also ($Da_1 = 0.35$, $Da_u = 0.5$). The scatter plots for $Da_u = 0.5$ and $Da_1 = 0.35$ are shown in Figs. 19 and 20, respectively. The IEM model result for $Da = 0.5$ shows a slightly higher degree of scatter which may be attributed to the non-local nature of the model. However, apart from this the IEM and EMST results are very similar for this case, and the critical Damköhler number predictions are in good agreement with the CMC result.

Moderate Reaction Zone Case: $\hat{\xi}_r = 1$

The CMC model prediction for the critical Damköhler number for $\hat{\xi}_r = 1$ is 56.02 (numerical parameters used to obtain this solution are shown in Table 7). The perturbation of the conditional mean progress variable from equilibrium (q_M) at Da_{crit} is shown in Fig. 21. The IEM prediction for this case is ($Da_1 = 1260$, $Da_u = 1500$), while the EMST prediction for this case is ($Da_1 = 122.5$, $Da_u = 175$). Both PDF models predict significantly higher critical Damköhler numbers than the CMC model. This may be due to the fact that in the CMC model spatial homogeneity is assumed, whereas in the

TABLE 6

Comparison of Stationary Values of $\langle y|\xi_R \rangle$ From the PDF Simulations Using IEM and EMST Models With the Mean Value of $q(\eta)$ in the Reaction Zone Obtained From CMC

	CMC	EMST	IEM
$\hat{\xi}_r = 10$			
$Da = 0.527$	0.14	0.066	0.075
$\hat{\xi}_r = 1$			
$Da = 2000$	2.5×10^{-4}		0.10
$Da = 175$	3.98×10^{-3}	1.03×10^{-2}	—
$\hat{\xi}_r = 0.27$			
$Da = 2000$	2.42×10^{-3}	9.98×10^{-4}	—

TABLE 7

Summary of Numerical Parameters for Each Case in the CMC Solution

	$\hat{\xi}_r = 10$	$\hat{\xi}_r = 1$	$\hat{\xi}_r = 0.27$
N —number of grid points in $0 \leq \eta \leq 1$	240	240	240
N_r —number of grid points in $[\xi_s - \Delta\xi_r/2, \xi_s + \Delta\xi_r/2]$	169	71	81
ρ —grid density parameter	1.0	1.0	0.2
W —non-uniform grid width parameter	0.005	0.005	1×10^{-5}
$\Delta\eta_{\min}/\Delta\xi_c$ —resolution in mixture fraction space	6.28×10^{-3}	7.4×10^{-3}	2.99×10^{-3}

physical problem there is a “flame brush.” The PDF models contain the transport of progress variable flux in closed form and presumably constitute a better model of the physical problem. The difference between the IEM and EMST predictions can be traced to the fact that the IEM model is non-local in composition space, whereas the EMST model is local in composition space. The scatter plots for $Da = 1500$ and $Da = 1260$ using the IEM model are shown in Figs. 22 and 23, respectively. For the stable reaction case (Fig. 22), the IEM model suggests that the pdf in composition space in the reaction zone is composed of 3 distinct regions: (i) a δ -function at equilibrium, (ii) relatively low probability density regions close to equilibrium corresponding to reaction terms being dominant, and (iii) region of high probability density corresponding to a dynamic balance between reaction, mixing and transport. For the case corresponding to global extinction (Fig. 23), the particles are found to be collapsing to the $Y = 0$ line. The scatter plots for $Da_u = 175$ and $Da_1 = 122.5$ using the EMST model are shown in Figs. 24 and 25, respectively. In this case for

stable reaction, there is considerably less scatter of particles away from the equilibrium line. The EMST model consistently predicts higher $\langle Y | \xi_R \rangle$ for stable reaction compared to IEM for all the cases. For the extinguishing case (cf. Figs. 25 and 23), there is a significant difference between the EMST and IEM model behavior. As opposed to the uniform collapse from equilibrium seen in the IEM scatter plot, the EMST model shows distinctly different behavior depending on whether or not the particles are in the reaction zone in mixture fraction space. Within the reaction zone there is a balance between mixing and reaction, with transport moving reactive particles out of the reaction zone into cells where the mean composition $(\langle \xi \rangle, \langle Y \rangle)$ lies outside the reaction zone in composition space ($\xi \in [\xi_s - \Delta\xi_r/2, \xi_s + \Delta\xi_r/2]$, $Y \in [Y_b, Y_c(\xi)]$) (where Y_1 corresponds to $f(y) = 0.1$). In the IEM model these reactive particles are mixed toward the cell mean resulting in

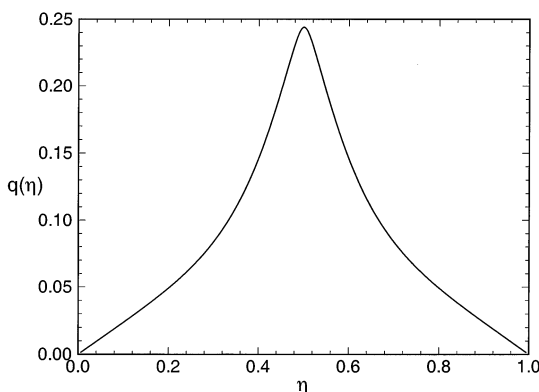


Fig. 16. Perturbation $q(\eta) = Y_c(\eta) - Q(\eta)$ obtained from the CMC model at $Da_{\text{crit}} = 0.527$ for the $\hat{\xi}_r = 10$ case.

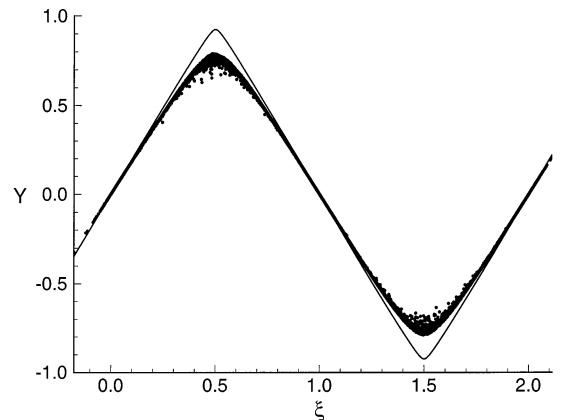


Fig. 17. Scatter plot of progress variable Y vs. mixture fraction ξ for the $\hat{\xi}_r = 10$ case at $t = 163$ ($2.8T_c$) using the IEM mixing model. The Damköhler number for this simulation ($Da = 0.5$) corresponds to stable reaction. The solid line is the equilibrium line $Y_c(\xi)$.

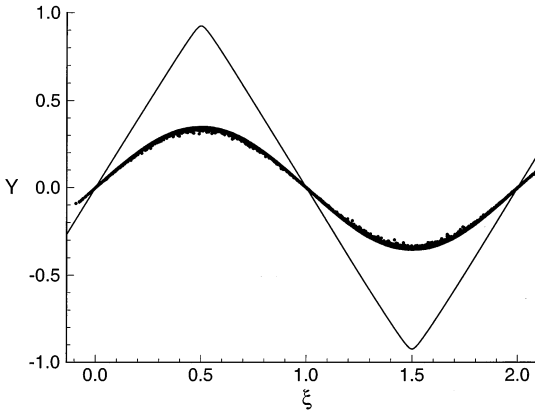


Fig. 18. Scatter plot of progress variable Y vs mixture fraction ξ for the $\xi_r = 10$ case at $t = 116.3 (2T_i)$ using the IEM mixing model. The Damköhler number for this simulation ($Da = 0.35$) corresponds to global extinction. The solid line is the equilibrium line $Y_c(\xi)$.

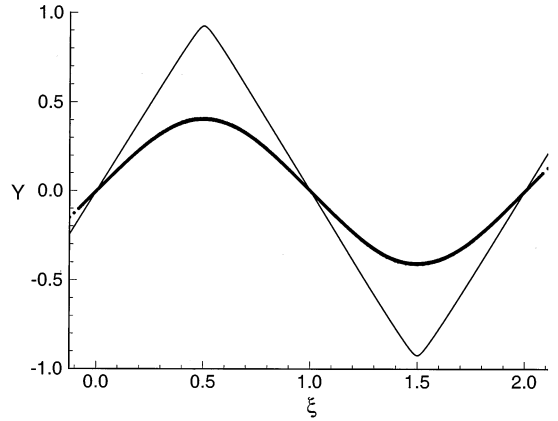


Fig. 20. Scatter plot of progress variable Y vs mixture fraction ξ for the $\xi_r = 10$ case at $t = 115.4 (1.98T_i)$ using the EMST mixing model. The Damköhler number for this simulation ($Da = 0.35$) corresponds to global extinction. The solid line is the equilibrium line $Y_c(\xi)$.

extinction at higher critical Damköhler numbers. In the EMST model, the reactive particles are mixed with their neighbors in composition space, and as a consequence they may remain in the reaction zone longer. This accounts for the lower critical Damköhler predictions which seem to be more consistent with the problem physics.

While the thermochemical model does exhibit the abrupt transition characteristic of flame extinction (as shown in Fig. 7), in the pdf simulations there is a range of Damköhler numbers, and only those particles whose Damköhler

number is close to the extinction value experience this abrupt transition corresponding to local extinction. When sufficiently many particles experience extinction, the criterion for global extinction is satisfied and the flame is deemed extinct. This transient phenomenon, which is also subject to statistical variability, cannot be inferred from scatter plots of instantaneous scalar values. In order to contrast the differences between the IEM and EMST models' particle trajectories in composition space just prior to global extinction, the scatter plots in Figs. 23 and 25 (and also Fig. 28) have been selected at output times prior to when all the particles are on the extinction ($Y = 0$) line. The later output times of those simulations would

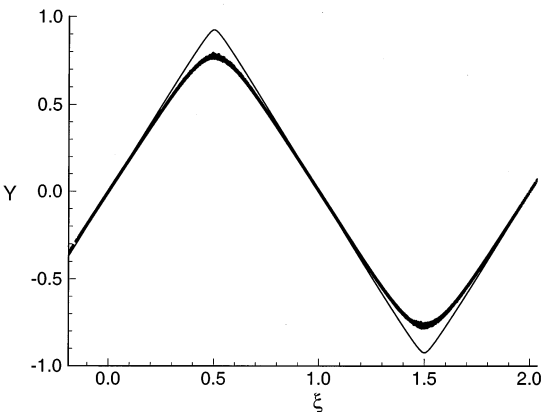


Fig. 19. Scatter plot of progress variable Y vs mixture fraction ξ for the $\xi_r = 10$ case at $t = 115.2 (1.98T_i)$ using the EMST mixing model. The Damköhler number for this simulation ($Da = 0.5$) corresponds to stable reaction. The solid line is the equilibrium line $Y_c(\xi)$.

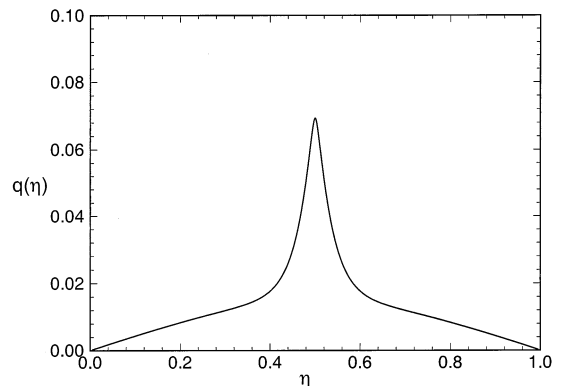


Fig. 21. Perturbation $q(\eta) = Y_c(\eta) - Q(\eta)$ obtained from the CMC model at $Da_{crit} = 56.02$ for the $\xi_r = 1$ case.

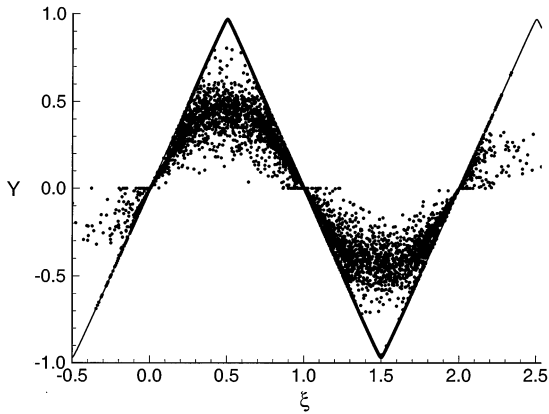


Fig. 22. Scatter plot of progress variable Y vs mixture fraction ξ for the $\hat{\xi}_r = 1$ case at $t = 15.7 (3T_1)$ using the IEM mixing model. The Damköhler number for this simulation ($Da = 1500$) corresponds to stable reaction. The solid line is the equilibrium line $Y_e(\xi)$.

only show all the particles on the extinction line, which does not provide information which is useful in comparing the models.

Thin Reaction Zone Case: $\hat{\xi}_r = 0.27$

The CMC model prediction for the critical Damköhler number for $\hat{\xi}_r = 0.27$ is 204.2 (see Fig. 26 and Table 7). This case constitutes a severe test for the PDF mixing models. The reaction zone in composition space is small and it is expected that reaction can be sustained only at Damköhler numbers higher than the CMC

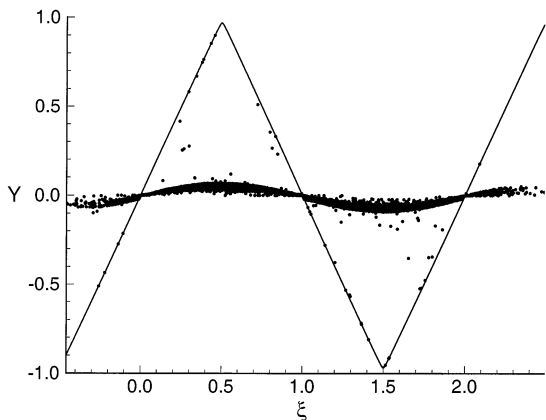


Fig. 23. Scatter plot of progress variable Y vs mixture fraction ξ for the $\hat{\xi}_r = 1$ case at $t = 19.8 (3.78T_1)$ using the IEM mixing model. The Damköhler number for this simulation ($Da = 1260$) corresponds to global extinction. The solid line is the equilibrium line $Y_e(\xi)$.

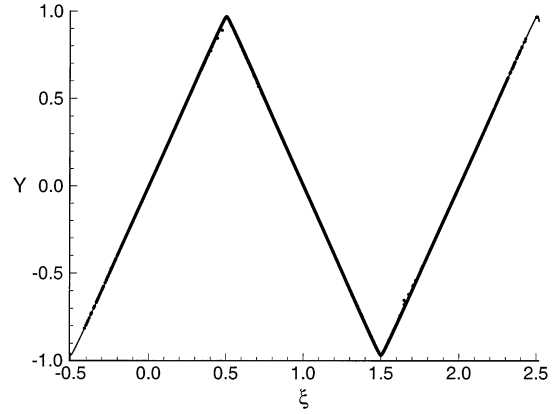


Fig. 24. Scatter plot of progress variable Y vs mixture fraction ξ for the $\hat{\xi}_r = 1$ case at $t = 15.67 (2.99T_1)$ using the EMST mixing model. The Damköhler number for this simulation ($Da = 500$) corresponds to stable reaction. The solid line is the equilibrium line $Y_e(\xi)$.

prediction. However, it is seen that while the EMST model prediction is within an order of magnitude of the CMC result, the IEM prediction is several orders of magnitude higher. For the IEM model, stable reaction could be sustained only at a Damköhler number of 1.6×10^6 . The EMST prediction for this case is ($Da_1 = 700$, $Da_u = 1000$). The scatter plot for stable reaction (Fig. 27) shows more particles departing from the equilibrium line compared to the stable reaction scatter plot for the moderate reaction zone thickness case (Fig. 24). This may

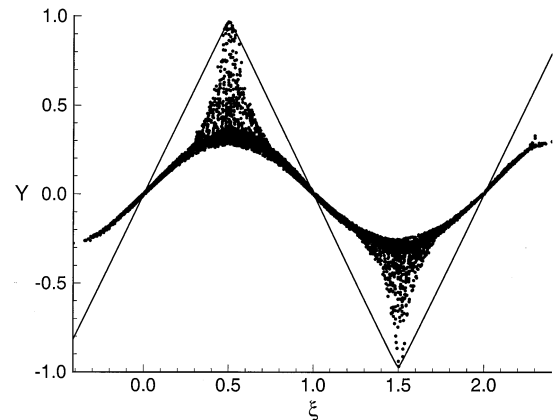


Fig. 25. Scatter plot of progress variable Y vs mixture fraction ξ for the $\hat{\xi}_r = 1$ case at $t = 7.77 (1.48T_1)$ using the EMST mixing model. The Damköhler number for this simulation ($Da = 122.5$) corresponds to global extinction. The solid line is the equilibrium line $Y_e(\xi)$.

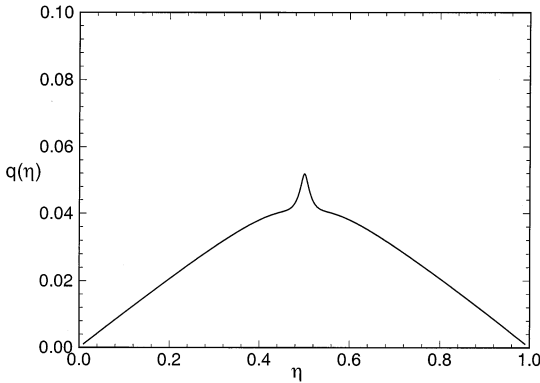


Fig. 26. Perturbation $q(\eta) = Y_c(\eta) - Q(\eta)$ obtained from the CMC model at $Da_{crit} = 204.2$ for the $\hat{\xi}_r = 0.27$ case.

be attributed to the fact that while the Damköhler number in the thin reaction zone scatter plot is equal to the upper bracket of the critical Damköhler number for that case ($Da_u = 1000$), the Damköhler number in the moderate reaction zone scatter plot ($Da = 500$ in Fig. 24) is higher than the upper bracket of the critical Damköhler number ($Da_u = 175$). The scatter plot corresponding to global extinction (Fig. 28) is not significantly different from the moderate reaction zone thickness case.

CONCLUSION

A model problem, periodic reaction zones, for studying turbulent nonpremixed reacting flow

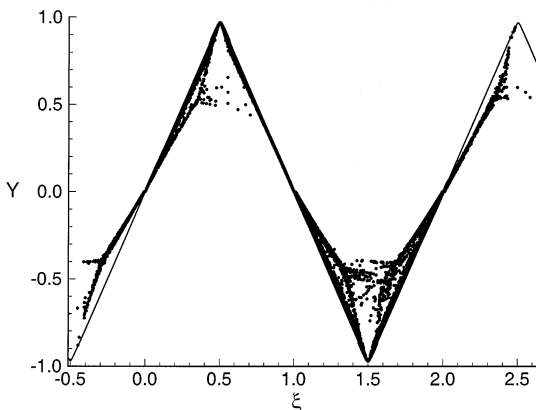


Fig. 27. Scatter plot of progress variable Y vs mixture fraction ξ for the $\hat{\xi}_r = 0.27$ case at $t = 10.87 (3T_i)$ using the EMST mixing model. The Damköhler number for this simulation ($Da = 1000$) corresponds to stable reaction. The solid line is the equilibrium line $Y_c(\xi)$.

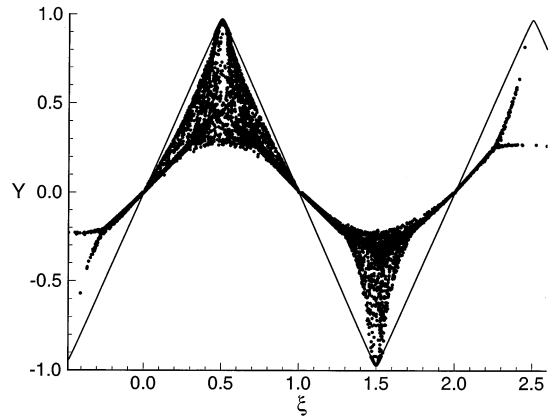


Fig. 28. Scatter plot of progress variable Y vs mixture fraction ξ for the $\hat{\xi}_r = 0.27$ case at $t = 7.29 (2T_i)$ using the EMST mixing model. The Damköhler number for this simulation ($Da = 700$) corresponds to global extinction. The solid line is the equilibrium line $Y_c(\xi)$.

has been developed, which admits stationary solutions that are periodic in physical space. Several important characteristics of turbulent flames are represented in this model problem, notably the presence of “flame-brush”-type solutions and a non-linear reaction rate function in composition space. For this simple problem, the different reacting flow regimes ranging from stable reaction to extinction may be characterized by points in the $Da-\hat{\xi}_r$ parameter space. A model thermochemistry is developed, which permits access to a broad range of values in this parameter space. The predictions of three different models of turbulent combustion are compared for three different values of the non-dimensional reaction zone thickness: corresponding to broad ($\hat{\xi}_r = 10$), moderate ($\hat{\xi}_r = 1$) and thin ($\hat{\xi}_r = 0.27$) reaction zones. The model predictions are in good agreement for the broad reaction zones, but considerable differences arise for the moderate and thin reaction zone cases. It is conjectured that the turbulent transport of progress variable could account for the differences between the CMC and PDF models. The differences in the PDF model predictions can be attributed to the fact that the IEM mixing model is non-local in composition space, whereas the EMST mixing model satisfies the localness property. It is found that in the range of moderate to thin reaction zones, violation of the localness princi-

ple can result in very significant differences in model predictions. It is believed that this localness principle provides a more physically accurate representation of mixing in such reactive flows and certainly the trend in the results is plausible. The PDF results obtained using the IEM and EMST mixing models are consistent with those obtained for piloted jet diffusion flames by Masri, Subramaniam and Pope [26], and suggest that EMST is more reliable than IEM at predicting global extinction.

While the DNS study of PRZ [11] could not access the same parameter range as the PDF simulations reported here, its results lend strong support to this hypothesis. The DNS study also shows that there is large spatial variability (or intermittency) in the scalar dissipation, which is instrumental in triggering local extinction. This indicates that, in order to predict local extinction, mixing models must include the effect of fluctuations in the scalar dissipation, as is done in Fox's spectral relaxation model [27].

This work was supported by the Air Force Office of Scientific Research, grant F49620-94-1-0098. The authors thank Dr. M. R. Overholt for permission to use a figure from his work.

REFERENCES

- Masri, A. R., Dibble, R. W., and Barlow, R. S., *Combust. Flame* 91:285 (1992).
- Chen, J.-Y., and Kollmann, W., *Twenty-Second Symposium (International) on Combustion*, The Combustion Institute, Pittsburgh, (1988), p. 645.
- Taing, S., Masri, A. R., and Pope, S. B., *Combust. Flame* 95:133 (1993).
- Norris, A. T., and Pope, S. B., *Combust. Flame* 100:211 (1995).
- Subramaniam, S., and Pope, S. B., *Combust. Flame* 115:487 (1998).
- Subramaniam, S., PhD thesis, Cornell University (1997).
- Lee, Y. Y., and Pope, S. B., *Combust. Flame* 101:501 (1995).
- Leonard, A. D., and Hill, J. C., *Phys. Fluids A* 3:1286 (May 1991).
- Overholt, M. R., and Pope, S. B., *Phys. Fluids A* 8:3128 (November 1996).
- Subramaniam, S., and Pope, S. B., Technical Report FDA 97-03, Cornell University (1997).
- Overholt, M. R., and Pope, S. B., Technical Report FDA 98-01, Cornell University (April 1998).
- Williams, F. A., *Combustion Theory*. Addison-Wesley, 2nd edition, 1985, p. 82.
- Bilger, R. W., *Phys. Fluids A* 5:436 (1993).
- Pope, S. B., *Prog. Energy Combust. Sci.* 11:119 (1985).
- Haworth, D. C., and Pope, S. B., *Phys. Fluids* 29:387 (1986).
- Pope, S. B., *Phys. Fluids* 6:973 (1986).
- Jayesh, and Pope, S. B., Technical Report FDA 95-05, Cornell University (Oct 1995).
- Chen, H., Chen, S., and Kraichnan, R. H., *Phys. Rev. Lett.* 63:2657 (Dec 1989).
- Pope, S. B., *Theoret. Comput. Fluid Dyn.* 2:255 (1991).
- Valiño, L., and Dopazo, C., *Phys. Fluids A* 3:3034 (1991).
- Dopazo, C., *Phys. Fluids* 18:397 (1975).
- Curl, R. L., *A.I.Ch.E.J.* 9(175) (1963).
- Norris, A. T., and Pope, S. B., *Combust. Flame* 83:27 (1991).
- Pope, S. B., PDF2DV: A FORTRAN code to solve the modeled joint pdf equations for two-dimensional recirculating flows. Unpublished, Cornell University.
- Yang, B., and Pope, S. B., *Combust. Flame* 112:16 (1998).
- Masri, A. R., Subramaniam, S., and Pope, S. B., A mixing model to improve the pdf simulation of turbulent diffusion flames. In *Twenty-Sixth Symposium (International) on Combustion*. The Combustion Institute, Pittsburgh (1996).
- Fox, R. O., *Phys. Fluids* 9:2364 (1997).

Received 27 January 1998; revised 10 September 1998; accepted 21 September 1998